Advance Publication

Journal of Clinical Biochemistry and Nutrition

Received: June 5, 2024 Accepted: August 14, 2024 Released online: August 24, 2024

DOI: https://doi.org/10.3164/jcbn.24-88

Original Article

Effective disruption of cancer cell membranes by photodynamic therapy with cell membrane-adhesive photosensitizer

Aoi Hoshi[1,2,†], Toru Yoshitomi[1,†,*], Yoshiki Komatsu[3], Naoki Kawazoe[1], Guoping Chen[1], Hiroko Bando[4], Hisato Hara[4], and Hirofumi Matsui[3,*]

[1] Research Center for Macromolecules and Biomaterials, National Institute for Materials Science, 1-1 Namiki, Tsukuba, Ibaraki 305-0044, Japan
[2] Graduate School of Comprehensive Human Sciences, University of Tsukuba, 1-1-1 Tennodai, Tsukuba, Ibaraki 305-8577, Japan
[3] Department of Gastroenterology, Institute of Medicine, University of Tsukuba, 1-1-1 Tennodai, Ibaraki 305-8575, Japan
[4] Department of of Breast and Endocrine Surgery, Institute of Medicine, University of Tsukuba, 1-1-1 Tennodai, Ibaraki 305-8575, Japan

[†]Equal contribution: A.H. and T.Y. contributed equally to this work.

*Corresponding authors:
Toru Yoshitomi
Research Center for Macromolecules and Biomaterials, National Institute for Materials Science, 1-1 Namiki, Tsukuba, Ibaraki 305-0044, Japan
YOSHITOMI.Toru@nims.go.jp (T.Y.)
Tel: +81-29-860-4739

Hirofumi Matsui
Department of Gastroenterology, Institute of Medicine, University of Tsukuba, 1-1-1 Tennodai, Ibaraki 305-8575, Japan
E-mail: hmatsui@md.tsukuba.ac.jp (H.M.)
Tel : +81-29-853-3466

Word count: 3056 words

Number of tables/figures: 7 figures

CRediT authorship contribution statement

Conceptualization, A.H., T.Y., and H.M.; **methodology,** A.H., and T.Y.; **validation,** A.H., and T.Y.; **formal analysis,** A.H. and T.Y.; **investigation,** A.H., and T.Y.; **resources,** T.Y., N.K., and G.C.; **data curation,** A.H., and T.Y.; **writing—original draft preparation,** A.H. and T.Y.; **writing—review and editing,** all coauthors; **visualization,** A.H. and T.Y.; **supervision,** T.Y. and H.M; **project administration,** T.Y.; **funding acquisition,** T.Y., N.K., G.C. and H.M. All authors have read and agreed to the published version of the manuscript.

Summary

Photodynamic therapy (PDT) is a noninvasive cancer treatment modality that involves the administration of photosensitizers and light irradiation. Previously, we established a polycation-containing hematoporphyrin (aHP) formulation that demonstrated superior antitumor efficacy *in vivo*, than the original hematoporphyrin (HP). In this study, we investigated underlining mechanisms of the high antitumor effect of aHP using cell experiments. Time-lapse imaging of rat gastric cancerous cell line (RGK45) treated with aHP exhibited swelling, cell rupture, and subsequent scattering of small vesicles upon light irradiation, in contrast to the small changes in morphology of RGK45 treated with HP. Furthermore, aHP presented concentrated localization on the cell membranes to a greater extent than HP. Additionally, neither aHP nor HP induced morphological changes in rat gastric mucosa cell line (RGM1). Flow cytometry analysis demonstrated a higher fluorescence of wheat germ agglutinin-conjugated dye in RGK45 than in RGM1, suggesting differential glycan expression patterns. These findings collectively suggest that the cellular toxicity of aHP may be augmented in RGK45 cells owing to its heightened affinity toward negatively charged structures on cellular membranes and its preferential localization on them. The observed membrane rupture and release of extracellular vesicles may confer an abscopal effect, in addition to direct PDT effect, thereby positioning aHP as a promising next-generation photosensitizer.

Keywords

photodynamic therapy; hematoporphyrin; polycation; cell adhesive; cellular membrane; glycan

Introduction

Photodynamic therapy (PDT) has the potential to be a non-invasive antitumor therapy owing to high spatiotemporal selectivity using a combination of photosensitizers and light irradiation.[1-4] Excited photosensitizers produce reactive oxygen species (ROS) that can induce tumor cell death via multiple mechanisms, including apoptosis, necrosis, and immunogenic cell death (ICD).[5-7] Among these, ICD has recently received great attention due to its ability to induce the abscopal effect.[7] The abscopal effect is triggered by several steps, i.e., (1) Photosensitizers in light-exposed cancer cells cause cell death, cell membrane disruption, and the release of damage-associated molecular patterns (DAMPs) from cells. (2) Macrophages and dendritic cells take up DAMPs released from lethal cancer cells and differentiate into antigen-presenting cells. (3) Antigen-presenting cells activate T cells, and cytotoxic T cells that recognize antigens and eliminate tumor cells in non-irradiated areas. DAMPs are endogenous molecules containing fragments of cellular membrane protein antigens.[8] Effective cellular damage caused by PDT induces abscopal effects via the release of DAMPs.[8] However, the efficiency of conventional photosensitizers in disrupting cell membranes remains controversial. Depending on the molecular design of photosensitizers, it may be possible to efficiently disrupt cell membranes.

Recently, for PDT with locally administered photosensitizer, we have developed a polycation-containing hematoporphyrin (aHP), which is composed of a copolymer of poly[2-(methacryloyloxy)ethyl]trimethylammonium chloride and poly[*N*-(3-aminopropyl)methacrylamide hydrochloride] conjugated with hematoporphyrin dihydrochloride (HP) (PMETAC-*co*-PAPMAA(HP)) (Fig.1).[9] The low-molecular-weight photosensitizer HP (Fig.1) does not remain in the tissue after local administration, whereas aHP is retained locally in the injected sites for one week after administration.[10] PDT using locally administered aHP allows multiple light irradiations through long-term retention at locally injected sites.[10] The cell membrane possesses negatively charged glycans on its surface and aHP may electrostatically adhere to these and cause cell rupture upon light irradiation. In a previous study, aHP-induced cell swelling was observed.[10] However, the underlining mechanisms of aHP on cancer cell swelling and rupture remain unclear. The aim of this study is to elucidate the mechanism by which aHP induces cancer cell toxicity, and to compare its potency to that of HP. Time-lapse imaging was performed using a laser confocal microscope to observe chronological changes in the destructing cell treated with aHP. Furthermore, as negatively charged glycans are expressed in both cancer and normal cells, the impact of PDT with aHP on cancer and normal cells was investigated using the rat gastric mucosal cancer cell line RGK45 and the rat gastric mucosal cell line RGM1.

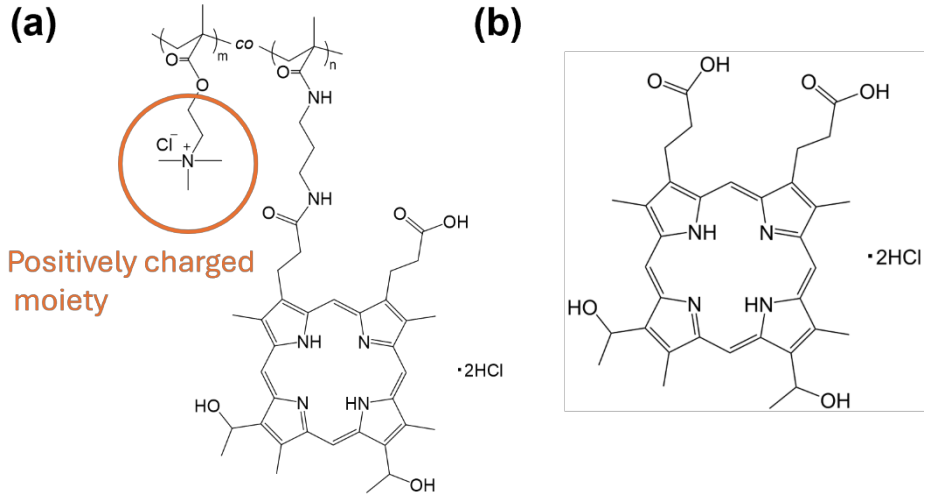

Fig. 1. Chemical structures of (a) aHP and (b) HP.

2. Materials and Method

2.1. Materials

RGM1 was purchased from RIKEN Cell Bank (Tsukuba, Japan). RGK45 cells were established by exposing 1-methyl-3-nitro-1-nitrosoguanidine to RGM1.[11] HP was purchased from MedChem Express (San Diego, CA, USA). Dulbecco's modified Eagle's medium/nutrient mixture F-12 Ham with 15 mM HEPES and sodium bicarbonate without L-glutamine and Dulbecco's Modified Eagle's Medium/Nutrient Mixture F-12 Ham with 15mM HEPES and sodium bicarbonate without L-glutamine and phenol red were purchased from Sigma-Aldrich (St. Louis, MO, USA). DMEM/F-12 with 15 mM HEPES and L-glutamine was purchased from Thermo Fischer Scientific (San Jose, CA, USA). DMEM/Ham's F-12 with L-glutamine, sodium pyruvate and HEPES, without phenol red was purchased from Nacalai Tesque (Kyoto, Japan). CellMask Deep Red Plasma Membrane Stain (CellMask), was purchased from Thermo Fischer Scientific (San Jose, CA, USA). Hoechst33342 was purchased from Dojindo (Kumamoto, Japan). CF488A-Wheat Germ Agglutinin (WGA) was purchased from Biotium (San Francisco, CA, USA).

2.2. Preparation of aHP

PMETAC-*co*-PAPMAA(HP) was prepared as previously reported.[9] To prepare a stock solution, aHP was dissolved in Phosphate Buffered Saline (PBS) and sterilized using filters with pore size of 0.2 μm. UV–vis spectra of aHP and HP were collected using a UV-2600 UV-visible spectrophotometer (Shimadzu Corp., Japan).

2.3. Cell culture

To keep their viability high, RGM1 and RGK45 cells were cultured in DMEM/F12 with L-glutamine and DMEM/F12 without L-glutamine, respectively. The culture medium contained 10% inactivated fetal bovine serum (FBS) (Biowest LLC, Kansas City, MO, USA) and 1% penicillin/streptomycin (FUJIFILM Wako Pure Chemical Industries, Ltd., Osaka, Japan). As L-glutamine has no antioxidant activity, its effect on this experiment would be ignorable.

2.4. Time-lapse observation of cellular behavior using confocal microscope

The cells were seeded on 35 mm glass-bottom culture dishes at density of 3.0×10^3 cells per glass area and incubated overnight in a 5% CO_2 incubator at 37 °C. Subsequently, they were incubated at 4 °C for 1 h and washed once with cold PBS. Five hundred microliters of fresh cold medium without FBS/phenol red, containing HP or aHP (porphyrin concentration: 0.5 μM) and CellMask was added to the cells. The glass-bottom dish containing the cells was set on a STELLARIS 8 confocal microscope (Leica Microsystems, Wetzlar, Germany) equipped with a 5% CO_2 incubator at 37 °C, and time-lapse monitoring was initiated. The excitation wavelengths for porphyrin and CellMask were 560 and 660 nm, respectively. The laser powers measured using a silicon photodetector (PM160, Thorlabs, Bergkirchen, Germany) at 560 and 660 nm were 210 nW and 15 nW, respectively.

2.5. Local distribution of HP and aHP

RGK45 cells were seeded on 35 mm glass-bottom dishes at density of 3.0×10^3 cells per glass area and incubated overnight in the 5% CO_2 incubator at 37 °C. Subsequently, the cells were incubated at 4 °C for 1 h and washed once with cold PBS. Five hundred microliters of fresh

medium without FBS/phenol red, which contained HP or aHP (porphyrin concentration, 5 μM), CF488A-WGA (5 μg/mL), and Hoechst33342 (5 μg/mL), were added to the cells. The cells were observed under a Zeiss LSM 900-Airyscan-2 microscope (Zeiss, Jena, Germany) at 23 °C. 3D analysis of signal intensity was performed using Zen blue edition software (Zeiss). The excitation wavelengths for Hoechst33342, CF488A-WGA, and the porphyrins were 405, 488, and 568 nm, respectively.

2.6. WGA adherence to RGM and RGK cells

RGM1 and RGK45 cells were seeded in 6 cm culture dishes and incubated for 24 h. The cells were washed three times with PBS and harvested using 0.05% trypsin/EDTA solution. The cells were washed three times with PBS, and fresh medium without FBS/phenol red containing CF488A-WGA was added to the suspended cells. They were then incubated for 10 min at 23 °C and washed once with culture media. The cells were resuspended in medium and analyzed using a flow cytometer (BD Accuri™ C6 Plus System, BD Biosciences, CA, USA).

2.7. Statistical analysis

Statistical analyses between the two unpaired groups were conducted using Student's *t*-test (Microsoft Excel, Microsoft Corporation, WA, USA). Statistical significance was set at $p < 0.05$.

3. Results

3.1. Time-lapse imaging of RGK45 cells with HP or aHP

Cell rupture induced by aHP was observed using time-lapse imaging; cells were exposed to laser light from a confocal microscope connected to a 5% CO_2 incubator at 37 °C. Cell membranes were stained with CellMask for clear observation of the cell membrane. The CellMask is composed of amphiphilic molecules containing a negatively charged hydrophilic dye and a hydrophobic moiety that anchors the probe onto the cell membrane. The maximum absorption of CellMask is at 660 nm. The absorption spectra of aHP and HP were measured from 500 to 700 nm to determine the excitation wavelengths of aHP and HP in time-lapse imaging (Fig. 2). An

excitation wavelength of 560 nm was used for aHP and HP. To minimize the effect of CellMask on the cell membrane, the laser power at 560 and 660 nm was set to 210 and 15 nW, respectively.

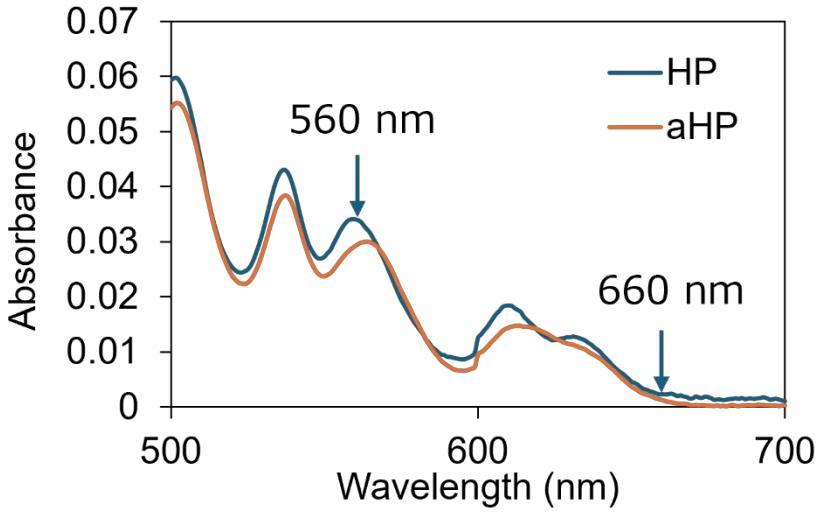

Fig. 2. Absorption spectra of aHP and HP in PBS from 500 to 700 nm. The concentration of porphyrin was 20 μM.

First, time-lapse imaging of the RGK45 cells was performed. As presented in Fig. 3a, staining with CellMask had little effect on the morphology of cell membranes of RGK45. In the time-lapse images of RGK45 cells treated with aHP, swelling of the cell membrane was observed (yellow dotted square in Fig. 3b) at the 38th scan. By the 60th scan, the swollen portion had ruptured. After the 38th scan, small extracellular vesicles were released in the vicinity (white arrowheads in the 38th and 60th scans in Fig. 3b). This result indicated that the cell membrane was destroyed by aHP upon light irradiation. In contrast, the cells treated with HP exhibited less pronounced changes (Fig. 3c).

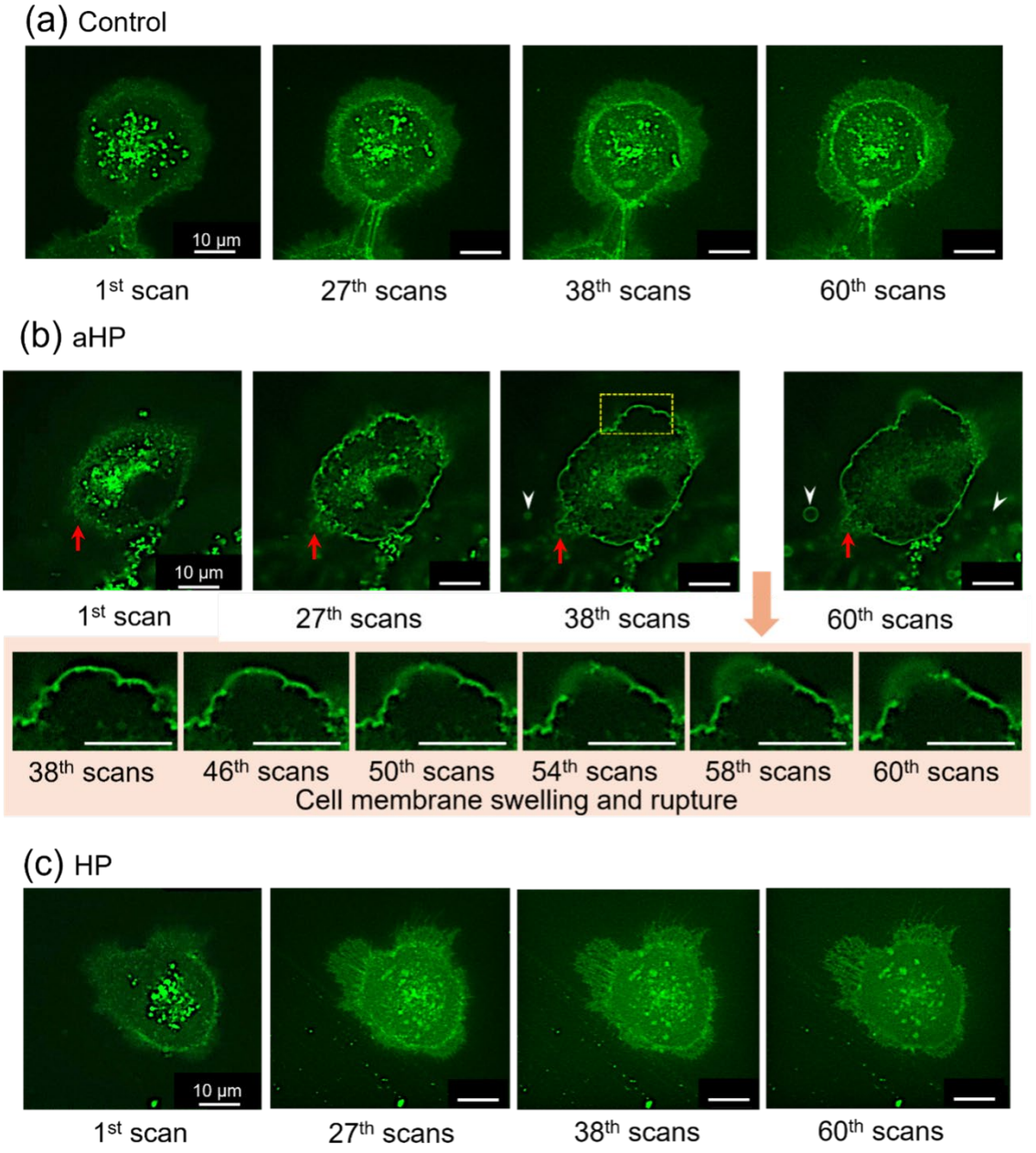

Fig. 3. Time-lapse images of RGK45 cells treated with (a) PBS, (b) aHP, and (c) HP upon the light irradiation by the laser scanner of confocal microscope at 560 nm. Cell membranes were stained with CellMask Deep Red Plasma Membrane Stain. In the fluorescence images, CellMask Deep Red Plasma Membrane Stain bound to cell membranes is shown in green. The porphyrin concentration in aHP and HP was 0.5 μM. White arrowheads indicate the released small extracellular vesicles by the cell disruption. Red arrows indicate a vesicle formed and released from the cell. At 27th scan, there was a "small bud" - like structure and its inflation was observed at 38th scan. At 60th scan, the small vesicle disappeared, and the attached membrane closed again.

3.2. Local distribution of HP and aHP

Time-lapse imaging revealed that aHP disrupted the cell membrane. Since aHP has positive charges, it may bind to the negatively charged glycans of glycoproteins or glycolipids present on the cell membrane, resulting in the oxidation of the cell membrane by ROS generation. The glycans on the cell membrane were stained with CF488A-WGA to confirm the intracellular localization of aHP. WGA is a lectin with a high affinity for sialic acid and N-acetylglucosamine moieties of glycoproteins and glycolipids in the cell membrane.[12-14] In the images of the RGK45 cells treated with PBS as a control, fluorescence signal of CF488A-WGA was detected on the cell membrane (Fig.4a). RGK45 cells treated with HP possessed strong fluorescence signals of porphyrin in their cytoplasm but did not show fluorescence signals on the membranes (Fig.4a). In contrast, the fluorescence signals from aHP were localized on the cell membrane as well as within the cytoplasm (Fig.4a). Strong aHP fluorescence signals were detected on the cell membrane in the area where WGA was stained (Fig. 4b), suggesting that aHP was electrostatically attached to glycans on the cell membrane.

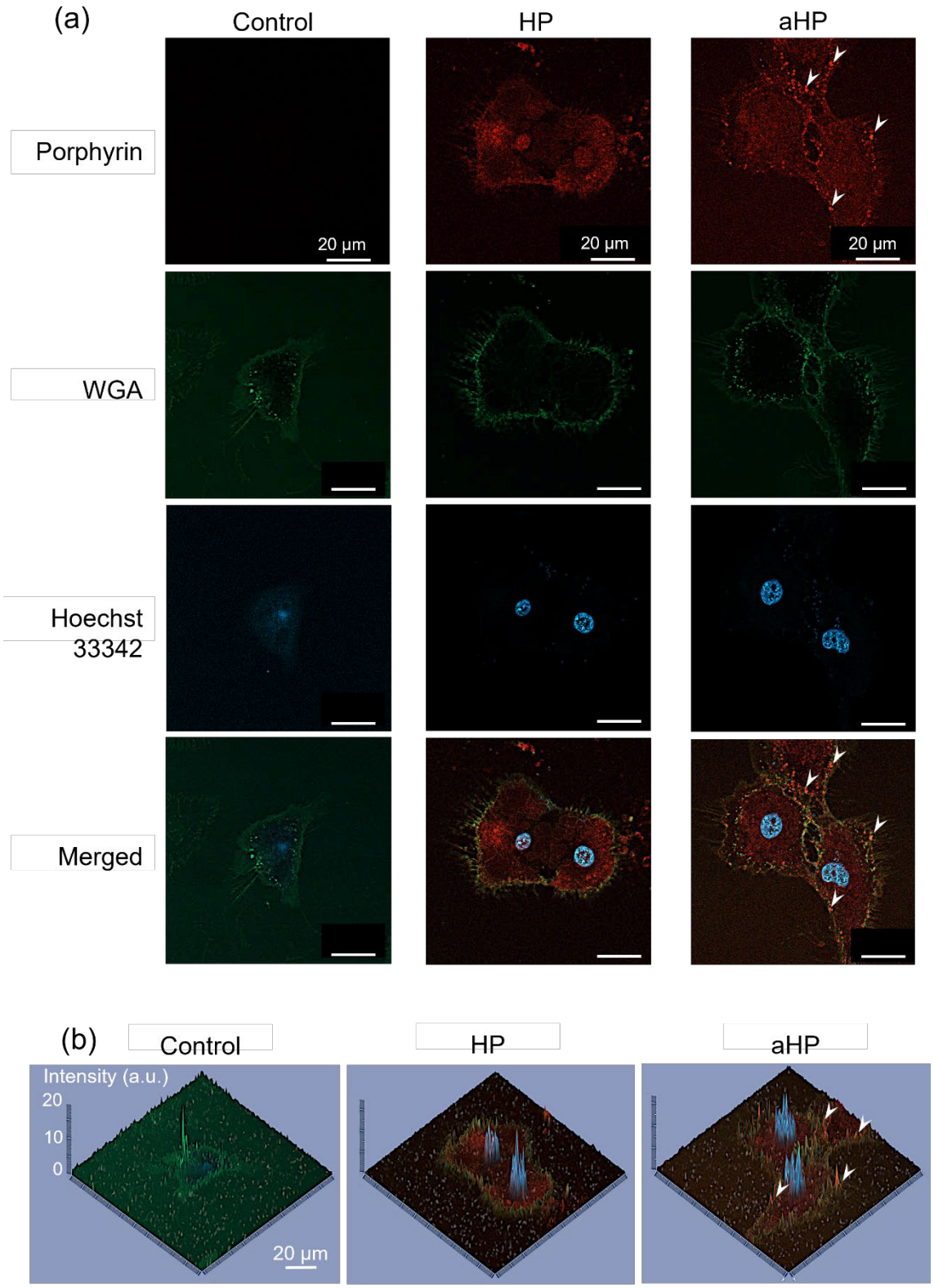

Fig. 4. Intracellular localization of HP and aHP in RGK cells. (a) Fluorescence images of RGK45 treated with CF488-WGA, Hoechst 33342 and HP or aHP. The glycan on the cell

membrane was stained with Wheat Germ Agglutinin (WGA), which are depicted in green. The nuclei were stained by Hoechst 33342, which are depicted in blue. The porphyrin is depicted in red. The porphyrin concentration in in HP and aHP was 5 μM. (b) 3D intensity plots of the fluorescence in the merged images, in which the porphyrin, the nuclei, and the glycan are depicted in red, blue, and green, respectively.

3.3. Time-lapse imaging of RGM1 cells with HP and aHP

It has been reported that cancer cells are more resistant to oxidative stress than normal cells.[15] Owing to rapid cell proliferation, cancer cells naturally produce large amounts of ROS. Therefore, they have a high antioxidant capacity to protect themselves from damage caused by oxidative stress.[16] The time-lapse imaging of normal cells, RGM1, treated with aHP exposed to a laser scanning confocal microscope equipped with a 5% CO_2 incubator at 37 °C was also conducted. Cell membrane rupture was not observed throughout the irradiation period (Fig.5a) (in contrast to the RGK45 cells). In contrast, RGM1 cells treated with HP exhibited minimal ballooning of the cellular membrane but did not enlarge sufficiently to rupture during irradiation (Fig.5b). This suggests that cell membrane destruction by aHP upon light irradiation results in cancer cell selectivity.

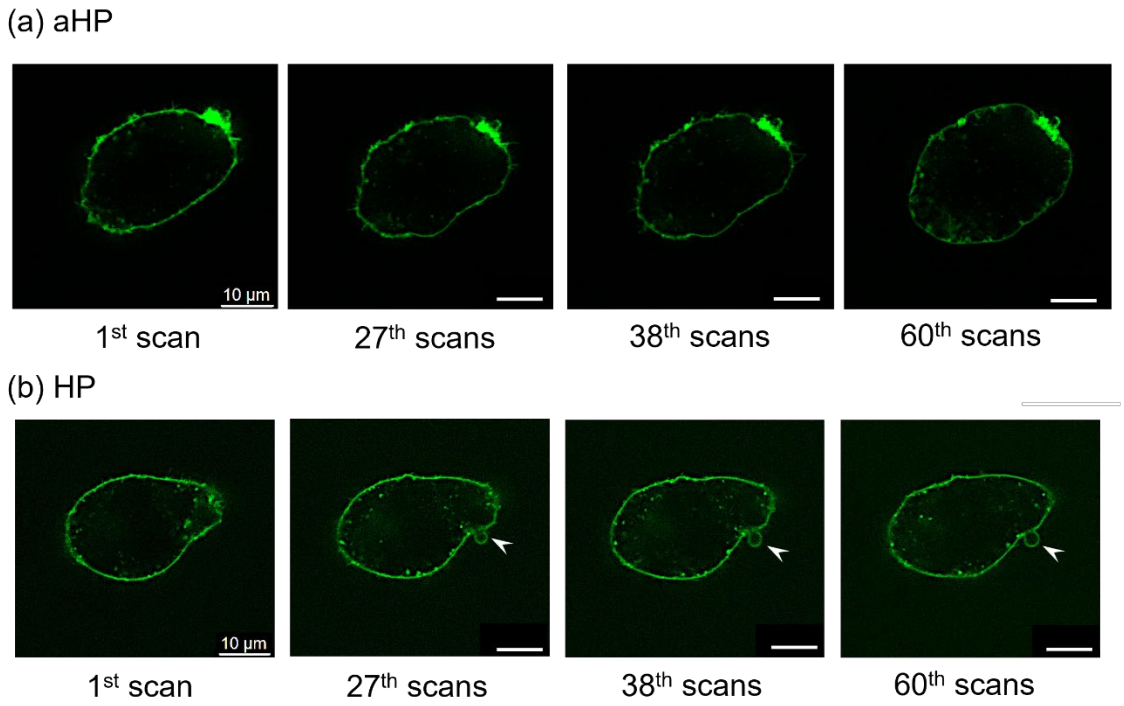

Fig. 5. Time-lapse images of RGM1 cells treated with (a) aHP and (b) HP upon light irradiation using the laser scanner of confocal microscope at 560 nm. Cell membranes were stained with CellMask Deep Red Plasma Membrane Stain. In the fluorescence images, CellMask Deep Red Plasma Membrane Stain bound to cell membranes is depicted in green. The porphyrin concentration in aHP or HP was 0.5 μM.

3.4. Comparison of the glycan amount on RGM1 and RGK45 cells using flowcytometry

The selective destruction of cancer cells by aHP upon light irradiation was explained by focusing on the disparities in the expression of glycan chains on the cell membranes of RGM1 and RGK45 cells. Staining of cells with CF488A-WGA allowed us to compare the glycan expression levels in RGM1 and RGK45 cells, which reflects the amount of aHP adhered to the cell membrane. Flow cytometry analysis revealed that the fluorescence intensity of CF488A-WGA was significantly higher in RGK45 cells than that in RGM1 cells ($p < 0.05$) (Fig.6). This result suggests that more aHP may adhere to glycan chains on the membranes of RGK45 cells than to those of RGM1 cells, thereby eliciting an exaggerated response in terms of cellular morphology (to light irradiation in

RGK45 cells).

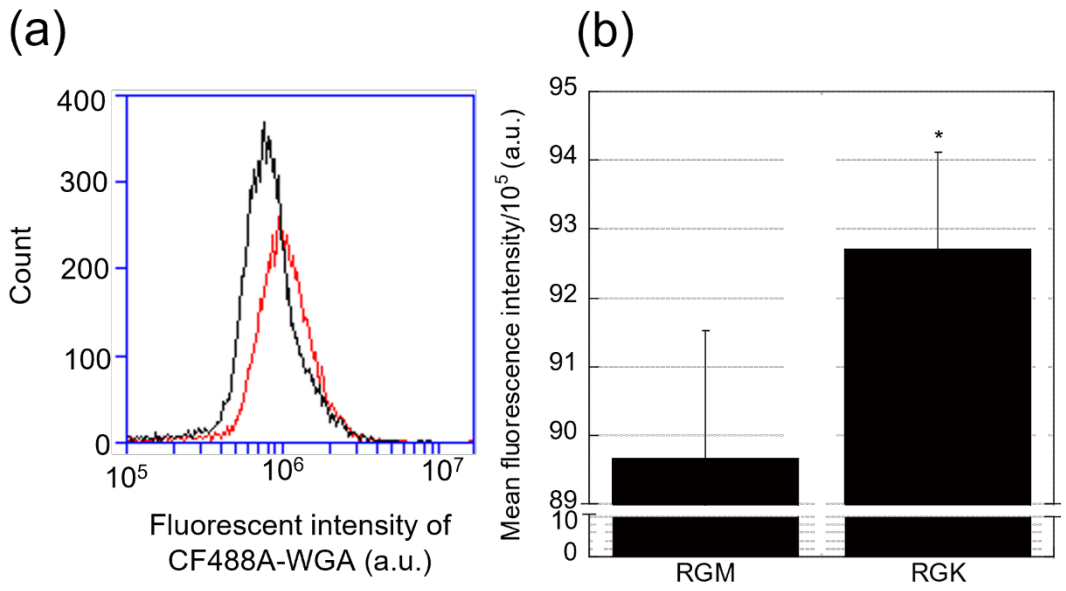

Fig. 6. Comparison of the glycan amount on RGM1 and RGK45 cells. (a) Flow cytometry histogram of the cells stained with CF®488A-WGA. Black: RGM1 cells; Red: RGK45 cells. (b) Mean fluorescence intensity of RGM and RGK stained with CF®488A-WGA. Data are presented as mean ± SEM (n=3). * $p < 0.05$

4. Discussion

We focused on PDT using locally administered photosensitizers and developed an aHP formulation as a local photosensitizer.[10] In PDT, as light irradiation is focused on the tumor tissue using an optical fiber, a photosensitizing agent can be administered locally in the tumor tissues or in the vicinity of the tumor.[10] Subsequently, light irradiation focused on the tumor tissue generates singlet oxygen, which kills the cancer cells. As conventional photosensitizers rapidly diffuse without adhering to tumor tissues or cancer cells after local administration, light cannot be irradiated multiple times. In contrast, aHP has a prolonged presence in the injected sites because of its tissue adhesive properties, and it provides PDT for a minimum of three days. Therefore, antitumor effect can be intensified by increasing the frequency of light irradiation. Furthermore, skin phototoxicity associated with systemic administration can be avoided as aHP

does not diffuse over the body after local injection [10]. However, owing to the tissue transmittance of light, PDT is only effective at a depth of approximately 1 cm when irradiated with light at 630 nm. Therefore, the efficiency of ICD is extremely important for its effectiveness even in deep-seated and metastatic cancer cells. To enhance the efficiency of ICD, it is necessary to improve the efficiency of cell membrane disruption and release of DAMPs.

In our previous study, we developed a cell culture dish equipped with a singlet oxygen-generating cell-adhesive glass substrate for the fundamental investigation of plasma membrane-targeted PDT and demonstrated cell rupture and release of extracellular vesicles.[17] Based on those results, we hypothesized that extracellular vesicles would also be produced in PDT with aHP and performed the time-lapse monitoring in this study. Time-lapse imaging clearly revealed that introducing a polycation containing a quaternary ammonium salt into HP caused effective cell membrane disruption (Fig. 7). In contrast, low-molecular-weight HP did not induce cell membrane rupture in RGK45 cells. HP localizes to whole cells, including the endoplasmic reticulum, mitochondria, golgi complex, lysosomes, and cell membrane.[18-20] Although some HP exist in the cell membrane, their presence is low. In contrast, aHP contains polycations with a number-average molecular weight of approximately 23,000. As cell membranes possess negatively charged glycans, aHP can adhere to the cell membrane. A higher density of aHP around the cell membrane effectively oxidizes the cell membrane, causing cell rupture. Therefore, the swelling and rupture of cancer cells were more pronounced in cells treated with aHP than in those treated with HP.

Additionally, small-sized extracellular vesicles were released from the cell membrane after treatment with aHP upon light irradiation (Fig. 7). Dendritic cells and macrophages engulf cancer cell fragments and differentiate into antigen-presenting cells, followed by the activation of cancer cell-specific cytotoxic T cells.[8] The small extracellular vesicles released from ruptured cells during PDT with aHP may be taken up by dendritic cells and macrophages and activate innate immunity. As the cellular membrane is damaged, DAMPs from within the cells must also be released. This results in an enhanced abscopal effect in comparison to PDT with HP. The protein glycosylation on the membrane of cancer cells is the most-widely occurring change, which means that similar effect of aHP can be expected against various type of cancer cells. Furthermore, the effects of PDT with aHP on cancer and normal cells were examined using RGM1 and RGK45 cells. PDT with aHP revealed selectivity toward cancer cells. As light leaks into normal tissues during PDT, this selectivity toward cancer cells is extremely important to avoid damaging normal tissues and causing ICD against normal tissues. In addition, the amount of expression of cell

membrane glycans depend on various intrinsic factors of the glycosylation process within a given cell or tissue type.[21] Therefore, it would be possible to predict the efficacy of PDT using aHP by examining the expression levels of glycans in the biopsy. Although this paper is limited to the results of cell experiments, it is necessary to confirm in the future whether aHP actually shows tumor selectivity and can effectively destroy cell membranes *in vivo*. Thus, aHP with adhesive properties have the potential to be a next-generation photosensitizer for locally administered PDT.

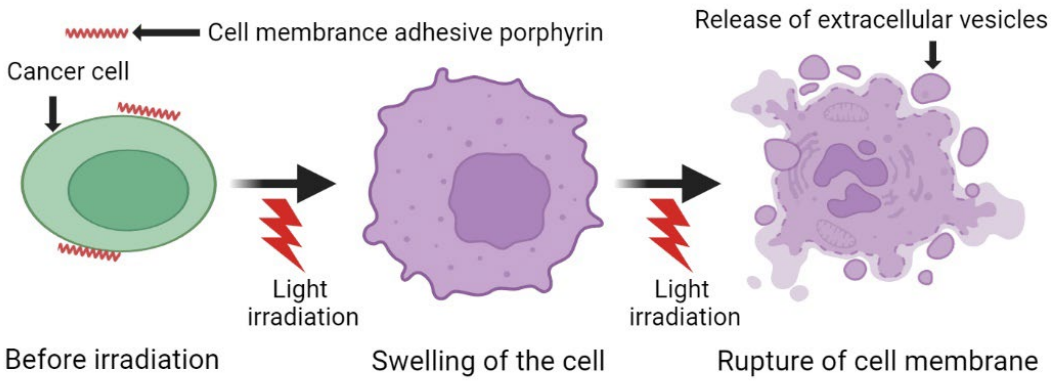

Fig. 7. Schematic illustration of cell rupture by PDT with aHP.

5. Conclusions

In this study, we demonstrated that aHP induces swelling and rupture in a rat gastric cancer cell line (RGK45) upon exposure to light, leading to the scattering of cellular membrane fragments and intracellular components in the vicinity. Conversely, treatment of the rat normal gastric mucosa cell (RGM1) with aHP resulted in less pronounced swelling and rupture. Additionally, we observed a disparity in the quantity of glycans in RGK45 and RGM1. Overall, these findings suggest that PDT using aHP selectively damages cancer cells *in vivo*. Although this phenomenon needs to be evaluated *in vivo*, exaggerated damage to cellular membranes may induce an abscopal effect, thereby enhancing the efficacy of PDT. These results suggest that PDT using locally

administered aHP has the potential to provide patients with cancer a less invasive and highly effective therapy than conventional PDT.

Conflict of Interest

No potential conflict of interest was reported by the author(s).

Acknowledgements

We thank the staff of Editage (https://www.editage.jp) for English language editing. Figure 7 was created using Biorender (https://biorender.com).

Funding

This research was supported by the Japan Society for the Promotion of Science KAKENHI [Grant number 21H03813].

References

1 Pham TC, Nguyen VN, Choi Y, Lee S, Yoon J. Recent Strategies to Develop Innovative Photosensitizers for Enhanced Photodynamic Therapy. *Chem Rev* 2021; **121**: 13454-13619.

2 Ito H, Matsui H. Mitochondrial Reactive Oxygen Species and Photodynamic Therapy. *Laser Ther* 2016; **25**: 193-199.

3 Li X, Lovell JF, Yoon J, Chen X. Clinical development and potential of photothermal and photodynamic therapies for cancer. *Nat Rev Clin Oncol* 2020; **17**: 657-674.

4 Kataoka H, Nishie H, Hayashi N*, et al*. New photodynamic therapy with next-generation photosensitizers. *Ann Transl Med* 2017; **5**: 183.

5 Chen ZA, Kuthati Y, Kankala RK*, et al*. Encapsulation of palladium porphyrin photosensitizer in layered metal oxide nanoparticles for photodynamic therapy against skin melanoma. *Science and Technology of Advanced Materials* 2015; **16**.

6 Bloyet C, Sciortino F, Matsushita Y*, et al*. Photosensitizer Encryption with Aggregation Enhanced Singlet Oxygen Production. *Journal of the American Chemical Society* 2022; **144**: 10830-10843.

7 Lou JY, Aragaki M, Bernards N*, et al*. Repeated photodynamic therapy mediates the abscopal effect through multiple innate and adaptive immune responses with and without immune checkpoint therapy. *Biomaterials* 2023; **292**.

8 Roh JS, Sohn DH. Damage-Associated Molecular Patterns in Inflammatory Diseases. *Immune Netw* 2018; **18**: e27.

9 Komatsu Y, Yoshitomi T, Furuya K*, et al*. Long-Term Fluorescent Tissue Marking Using Tissue-Adhesive Porphyrin with Polycations Consisting of Quaternary Ammonium Salt Groups. *Int J Mol Sci* 2022; **23**.

10 Komatsu Y, Yoshitomi T, Doan VTH*, et al*. Locally Administered Photodynamic Therapy for Cancer Using Nano-Adhesive Photosensitizer. *Pharmaceutics* 2023; **15**.

11 Shimokawa O, Matsui H, Nagano Y*, et al*. Neoplastic transformation and induction of H+,K+ -adenosine triphosphatase by N-methyl-N'-nitro-N-nitrosoguanidine in the gastric epithelial RGM-1 cell line. *In Vitro Cell Dev Biol Anim* 2008; **44**: 26-30.

12 Chazotte B. Labeling membrane glycoproteins or glycolipids with fluorescent wheat germ agglutinin. *Cold Spring Harb Protoc* 2011; **2011**: pdb prot5623.

13 Ashraf S, Qadri S, Akbar S, Parray A, Haik Y. Biogenesis of Exosomes Laden with Metallic Silver-Copper Nanoparticles Liaised by Wheat Germ Agglutinin for Targeted Delivery of Therapeutics to Breast Cancer. *Advanced Biology* 2022; **6**.

14 Fitzgerald LA, Denny JB, Baumbach GA, Ketcham CM, Roberts RM. Effect of altered oligosaccharide structure on the cell surface number, distribution and turnover of the high molecular weight acidic glycoproteins of CHO cells. *J Cell Sci* 1984; **67**: 1-23.

15 Trachootham D, Alexandre J, Huang P. Targeting cancer cells by ROS-mediated mechanisms: a radical therapeutic approach? *Nat Rev Drug Discov* 2009; **8**: 579-591.

16 Lee HY, Parkinson EI, Granchi C*, et al*. Reactive Oxygen Species Synergize To Potently and Selectively Induce Cancer Cell Death. *ACS Chem Biol* 2017; **12**: 1416-1424.

17 Doan VTH, Komatsu Y, Matsui H, Kawazoe N, Chen G, Yoshitomi T. Singlet oxygen-generating cell-adhesive glass surfaces for the fundamental investigation of plasma membrane-targeted photodynamic therapy. *Free Radic Biol Med* 2023; **207**: 239-246.

18 Ito H, Matsui H, Tamura M, Majima HJ, Indo HP, Hyodo I. Mitochondrial reactive oxygen species accelerate the expression of heme carrier protein 1 and enhance photodynamic cancer therapy effect. *J Clin Biochem Nutr* 2014; **55**: 67-71.

19 Kurokawa H, Ito H, Terasaki M*, et al*. Nitric oxide regulates the expression of heme carrier protein-1 via hypoxia inducible factor-1alpha stabilization. *PLoS One* 2019; **14**: e0222074.

20 Maharjan PS, Bhattarai HK. Singlet Oxygen, Photodynamic Therapy, and Mechanisms of Cancer Cell Death. *J Oncol* 2022; **2022**: 7211485.

21 Pinho SS, Reis CA. Glycosylation in cancer: mechanisms and clinical implications. *Nature Reviews Cancer* 2015; **15**: 540-555.

Figure legends

Fig. 1. Chemical structures of aHP and HP.

Fig. 2. Absorption spectra of aHP and HP in PBS from 500 to 700 nm. The concentration of porphyrin was 20 μM.

Fig. 3. Time-lapse images of RGK45 cells treated with (a) PBS, (b) aHP, and (c) HP upon the light irradiation by the laser scanner of confocal microscope at 560 nm. Cell membranes were stained with CellMask Deep Red Plasma Membrane Stain. In the fluorescence images, CellMask Deep Red Plasma Membrane Stain bound to cell membranes is shown in green. The porphyrin concentration in aHP and HP was 0.5 μM. White arrowheads indicate the released small extracellular vesicles by the cell disruption. Red arrows indicate a vesicle formed and released from the cell. At 27^{th} scan, there was a "small bud" - like structure and its inflation was observed at 38^{th} scan. At 60^{th} scan, the small vesicle disappeared, and the attached membrane closed again.

Fig. 4. Intracellular localization of HP and aHP in RGK cells. (a) Fluorescence images of RGK45 treated with CF488-WGA, Hoechst 33342 and HP or aHP. The glycan on the cell membrane was stained with Wheat Germ Agglutinin (WGA), which are depicted in green. The nuclei were stained by Hoechst 33342, which are depicted in blue. The porphyrin is depicted in red. The porphyrin concentration in in HP and aHP was 5 μM. (b) 3D intensity plots of the fluorescence in the merged images, in which the porphyrin, the nuclei, and the glycan are depicted in red, blue, and green, respectively.

Fig. 5. Time-lapse images of RGM1 cells treated with (a) aHP and (b) HP upon light irradiation using the laser scanner of confocal microscope at 560 nm. Cell membranes were stained with CellMask Deep Red Plasma Membrane Stain. In the fluorescence images, CellMask Deep Red Plasma Membrane Stain bound to cell membranes is depicted in green. The porphyrin concentration in aHP or HP was 0.5 μM.

Fig. 6. Comparison of the glycan amount on RGM1 and RGK45 cells. (a) Flow cytometry histogram of the cells stained with CF®488A-WGA. Black: RGM1 cells; Red: RGK45 cells. (b) Mean fluorescence intensity of RGM and RGK stained with CF®488A-WGA. Data are presented as mean ± SEM (n=3). * $p < 0.05$

Fig. 7. Schematic illustration of cell rupture by PDT with aHP.